

Visible-Light-Driven Photocatalytic Degradation of Rhodamine B over Bimetallic Cu/Ti-MOFs

Hong Tham Thi Nguyen^{1,2}, Kim Ngan Thi Tran^{1,2}, Thuy Bich Tran³, Thanh Trung Nguyen^{4,5}, Sy Trung Do⁶, and Kim Oanh Thi Nguyen^{1,2*}

¹Institute of Environmental Technology and Sustainable Development, Nguyen Tat Thanh University, 298-300A Nguyen Tat Thanh, Ward 13, District 4, Ho Chi Minh City, 700000, Vietnam

²Faculty of Food and Environmental Engineering, Nguyen Tat Thanh University, 298-300A Nguyen Tat Thanh, Ward 13, District 4, Ho Chi Minh City, 700000, Vietnam

³Institute of Environmental Science, Engineering and Management, Industrial University of Ho Chi Minh City, 12 Nguyen Van Bao Street, Ward 4, Go Vap District, Ho Chi Minh City, Vietnam

⁴Nanomaterial Laboratory, An Giang University, 18 Ung Van Khienn St., Dong Xuyen Dist, Long Xuyen City, An Giang Province, Vietnam

⁵Vietnam National University Ho Chi Minh City, Linh Trung Ward, Thu Duc District, Ho Chi Minh City, Vietnam

⁶Institute of Chemistry, Vietnam Academy of Science and Technology (VAST), Hanoi City, Vietnam

* **Corresponding author:**

tel: +84-392073898

email: ntkoanh@ntt.edu.vn

Received: October 13, 2021

Accepted: December 15, 2021

DOI: 10.22146/ijc.69765

Abstract: The first copper-doped titanium-based amine-dicarboxylate metal-organic framework was synthesized by the solvothermal approach in this article, with a Cu²⁺/Ti⁴⁺ ratio of 0.15 (15% Cu/Ti-MOFs). X-ray diffraction (XRD), Fourier transform infrared spectroscopy (FTIR), Raman spectra, N₂ adsorption-desorption studies, and UV-Vis diffuse reflectance spectroscopy (UV-Vis DRS) were all used to identify the crystalline and properties of the semiconductors. The rate constants of 15% Cu/Ti-MOFs to degrade Rhodamine B (RhB) were roughly two times higher than NH₂-Ti-MOFs. Furthermore, 15% Cu/Ti-MOFs photocatalysts remained stable after three cycles. The trapping test revealed that the principal active species in the degradation performance were hydroxyl radicals and holes.

Keywords: bimetallic Cu/Ti-MOFs; photocatalytic; degradation; Rhodamine B; kinetic

■ INTRODUCTION

Organic dyes have been widely used in the textile and print industries. However, because these compounds are toxic, non-biodegradable, and potentially carcinogenic, their release into the water supply could endanger humans and the environment [1]. Rhodamine B (RhB) is an example of a highly toxic dye [2]. Nonetheless, RhB is still used as a fluorescent dye for staining in biology, sometimes in conjunction with auramine O to form the auramine-rhodamine stain [3]. As a result, there is a pressing need to design an effective dye wastewater treatment process.

Metal-organic frameworks (MOFs) have many possible uses due to their huge surface areas, homogeneous yet configurable cavities, and tailorable physicochemical features [4-6]. Gas adsorption and storage [7], separation [8], drug delivery [9], and catalysis [10] are a few typical examples. In addition, the cost-effective photocatalysis process has gained popularity due to its advantages, such as biodegradable and non-toxic end products.

Recently, the photoactive, crystalline, and highly porous titanium-oriented MOFs NH₂-MIL-125(Ti) exhibiting Ti₈O₈(OH)₄(O₂CC₆H₃(NH₂)CO₂)₆ have

received much attention in the photocatalysis domain [11-13]. $\text{NH}_2\text{-MIL-125(Ti)}$ is crystal titanium-based amine-dicarboxylate with excellent absorbance, encapsulation potential, and stability [14]. This material is also embellished with numerous inactive Ti sites. However, due to its exclusive activation in the UV light area and quick charge recombination, its employment in photocatalytic platforms is limited, resulting in poor photocatalytic efficiency [15].

When suitable energy light strikes the photocatalyst, the generated electron-hole pair participates in the reaction [16]. Electron-hole pair recombination must be avoided to be so large to promote photocatalysis. The photocatalytic activity of MOFs has been improved using various techniques, including coupling with noble metals [17-18] and forming heterojunctions with other semiconductors [19-20]. Furthermore, metal doping is a potential method for regulating the electronic structure and improving photocatalytic activity. For example, Hong Liu et al. used an in situ doping approach to create new copper-doped titanium-based amine-functionalized metal-organic frameworks ($\text{Cu-NH}_2\text{-MIL-125(Ti)}$).

In this work, the photocatalytic activity of produced samples was demonstrated through the degradation of methyl orange (MO) and phenol under visible light [21]. In 2019, Gómez-Avilés et al. synthesized mixed Ti-Zr-MOFs and tested them as photocatalysts under solar-simulated radiation using acetaminophen (ACE) as a target pollutant [22]. However, a full comprehensive determination of the structure and photocatalysis mechanism of these materials remains challenging. The photocatalytic performance of bimetallics strongly depends on their composition and microstructures. Herein, the scope for further investigation into the role played by Cu^{2+} in $\text{NH}_2\text{-MIL-125(Ti)}$, which is also rare recently.

This article reports a simple method of synthesizing $\text{NH}_2\text{-Ti-MOFs}$ and bimetallic 15% Cu/Ti-MOFs using the solvothermal method. The bare Ti-MOFs were prepared to compare with 15% Cu/Ti-MOFs to highlight the advantage of transition metal-based on its superior optical performance. Moreover, Cu^{2+} was also supposed to play a part in the structural adjustment of $\text{NH}_2\text{-Ti-MOFs}$.

■ EXPERIMENTAL SECTION

Materials

Titanium (IV) isopropoxide ($\text{TiOCH}(\text{CH}_3)_2$), 2-amino terephthalic acid ($\text{NH}_2\text{-BDC}$) were purchased from Sigma-Aldrich Co. (St. Louis, MO, USA), copper(II) chloride (CuCl_2) were obtained from Fisher Scientific (Fair Long, NJ, USA), N-dimethylformamide (DMF, 99.5%) and methanol (CH_3OH) were obtained from Xilong Chemical Co., Ltd (China).

Instrumentation

The catalysts were identified using the powder X-ray diffraction (PXRD) technique, which used a 600 XRD diffractometer (Shimadzu, Japan) with Cu K α radiation ($\lambda = 1.5418$) at a scan rate of $0.020^\circ/\text{s}$ in the 5–40 range of the 2-theta range. Raman spectroscopy was performed using a HORIBA Jobin Yvon spectrometer (Horiba Scientific, Japan) with a wavenumber range of $100\text{--}1000\text{ cm}^{-1}$ (633 nm of the laser beam). FTIR spectroscopy was performed on the sample KBr pellets using a Jasco-4700 FTIR Spectrometric Analyzer (Japan). Nitrogen physisorption was used to investigate the BET and pore size distributions using a Micromeritics Tristar 3000 analyzer. The UV-vis DRS was measured at wavelengths ranging from 200 to 800 nm (UV-2450, Shimadzu, Japan).

Procedure

Preparation of $\text{NH}_2\text{-Ti-MOFs}$ and 15% Cu/Ti-MOFs

$\text{NH}_2\text{-Ti-MOFs}$ were synthesized via the report of Hanna et al. (2020) [23]. Briefly, 0.504 g 2-amino-1,4-benzene dicarboxylate (BDC-NH_2) was dissolved in 12.1 mL N,N-dimethylformamide (DMF). 1.4 mL methanol was added to the mixture and magnetically stirred at room temperature for 30 min. Next, 0.26 mL of titanium isopropoxide was added to the mixture, with continued stirring until homogenous, and later added with 20 mg of CTAB surfactant. Then, the reaction mixture was transferred to a heat-resistant 100 mL Teflon and placed in a closed convection heat apparatus at $150\text{ }^\circ\text{C}$ for 24 h. The product was then cooled and refluxed overnight at $80\text{ }^\circ\text{C}$ to remove BDC-NH_2 from the pores. Next, the obtained material was centrifuged,

washed several times with DMF and methanol, and vacuum dried overnight at 150 °C. The mixed Cu/Ti-MOFs were synthesized according to the copper molar percentage of the ratio $\text{Cu}^{2+}/\text{Ti}^{4+}$ of 0.15.

Photocatalytic test

The ability of $\text{NH}_2\text{-Ti-MOFs}$ and 15% Cu/Ti-MOFs samples to degrade RhB with the help of H_2O_2 and the presence of visible light demonstrates their photocatalytic activity. The catalyst (5 mg) was combined with RhB (100 mL, 3×10^{-5} M) and 1 mL H_2O_2 (2 mM) in a 250 mL double-layer beaker. Before photocatalytic degradation, the suspensions were magnetically stirred for 1 h without light to achieve equilibrium adsorption and desorption. Herein, 4 mL of samples were removed during the photodegradation process and centrifuged at 6000 rpm at regular intervals for 10 min to separate the solid material. An Agilent Cary (USA) was used to measure dye concentration and absorption.

Trapping test

The RhB photodegradation of 15% Cu/Ti-MOFs was conducted using different scavenger compounds to obtain in-depth knowledge about the photocatalytic reaction mechanism. $\text{O}_2^{\cdot-}$, HO^{\cdot} and h^+ scavengers were inhibited by p-benzoquinone (BQ), tert-butanol (TBA), and EDTA-2Na, respectively. The concentrations of TBA and EDTA were fixed at 1 mM, while the concentration of BQ was fixed at 1 μM .

■ RESULTS AND DISCUSSION

Characterization of $\text{NH}_2\text{-Ti-MOFs}$ and 15% Cu/Ti-MOFs

The XRD patterns of $\text{NH}_2\text{-Ti-MOFs}$ and 15% Cu/Ti-MOFs are shown in Fig. 1(a). The diffraction peak intensity at $2\theta = 6.8^\circ$ is attributed to the $\text{NH}_2\text{-Ti-MOFs}$ bare [24-25]. Noticeably, the diffraction peaks are slightly moved to lower angles when doping with ionic Cu^{2+} into the titanium framework. This can be explained based on the difference of the ionic radius of Cu^{2+} and Ti^{4+} which are 0.72 and 0.68 Å, respectively [21]. The slight decrease observed is probably due to the thermal treatment following metal deposition [26]. However, the modification of ion Cu^{2+} had not changed the crystalline phase of $\text{NH}_2\text{-Ti-MOFs}$.

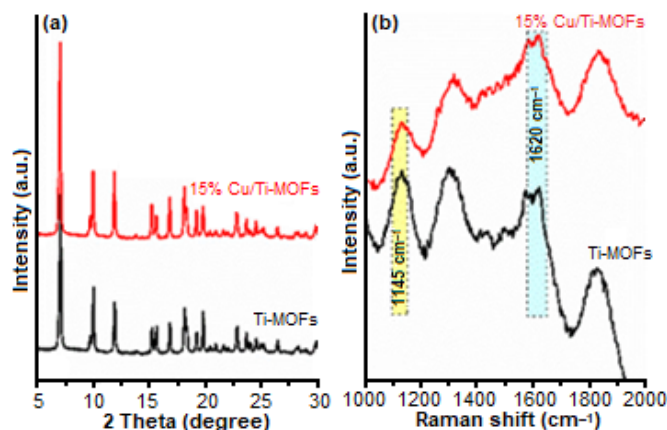


Fig 1. XRD pattern (a) and Raman spectra (b) of $\text{NH}_2\text{-Ti-MOFs}$ and 15% Cu/Ti-MOFs

Therefore, the formation of 15% Cu/Ti-MOFs was further confirmed.

Raman spectroscopy was used to investigate the bonding vibration of Ti-MOFs and 15% Cu/Ti-MOFs bimetallic materials (Fig. 1(b)). All of the spectra had the same characteristic peaks. The relatively strong bands observed at 325 nm at 546, 640, 1145, and 1620 cm^{-1} characterize $\text{NH}_2\text{-MIL-125(Ti)}$ materials [27]. The type of framework of titanium is responsible for the resonance-enhanced Raman band at 703 cm^{-1} . The N-H bond of the organic bridge is represented in the band at 1620 cm^{-1} [28]. The appearance of a band of symmetrical bending and elongation at 546 cm^{-1} is typical for octahedral Ti-O-Ti-O [29].

The nitrogen adsorption/desorption analyses at 77 K were used to explore the specific surface areas and porosity of MOF materials. As displayed in Fig. 2, all the samples exhibit the typical isotherms of IV, indicative of the presence of a large number of micropores with some small contribution of mesoporosity and high surface area values. The Brunauer-Emmett-Teller (BET) surface areas of the as-prepared $\text{NH}_2\text{-Ti-MOFs}$ and 15% Cu/Ti-MOFs were 970.23 and 1157.41 m^2/g , respectively. Therefore, as in the case of the crystalline structure, metal cluster modification did not provoke significant changes in the porous texture of the original $\text{NH}_2\text{-Ti-MOFs}$.

The UV-Vis spectra of $\text{NH}_2\text{-Ti-MOFs}$ reveal two prominent absorption bands with maxima at 217 and 370 nm, which are caused by the Ti-O and ligand cluster transition. Furthermore, an absorption band extending

up to 500 nm can be observed due to the NH_2 -BDC ligand [30]. After incorporating transition metals into Ti-MOFs, the UV-Vis absorption band redshifted, and the visible region expanded noticeably (Fig. 3(a)). The bandgap energy of all obtained samples was calculated using the graph of $(h\nu)^2$ versus photon energy (h) shown in Fig. 3(b). The bandgap of NH_2 -Ti-MOFs and 15% Cu/Ti-MOFs were calculated from the absorption line intersection and are 2.56 and 2.42 eV, respectively.

Photocatalytic Test

The photocatalyst efficiency of the as-prepared samples was figured out via the degradation of Rhodamine B (RhB) dye under visible light irradiation (Fig. 4(a)). It was found that the rate of degradation of NH_2 -Ti-MOFs was prolonged after 120 min of irradiation. However, the degradation process significantly rose when doping Cu^{2+} ions into the NH_2 -Ti-MOFs. Therefore, it is indicated that the Cu^{2+} ion helped the bandgap energy to narrow, which boosted the photocatalyst effect. Furthermore, as per the literature, $\cdot\text{OH}$ radicals were generated and acted as electron acceptors, which is the main factor in helping the MOFs generate more holes and encourage the photocatalysis process.

The kinetics of RhB degradation on NH_2 -Ti-MOFs and bimetallic 15% Cu/Ti-MOFs were also described via the pseudo-first-order (Fig. 4(b)). For 15% Cu/Ti-MOFs, the correlation coefficient (R^2) and the rate constant (k_1) for the pseudo-first-order kinetic model were the highest. Notably, the kinetic rate of 15% Cu/Ti-MOFs reached

10.23 (10^{-3} min^{-1}), which showed the highest photocatalytic performance. The UV-Vis absorption spectra of RhB to irradiation time over Ti-MOFs and 15% Cu/Ti-MOFs are also depicted in Fig. 4(c-d). The RhB dye solution's absorption peak was at 554 nm, and it gradually decreased due to dye degradation, reaching its lowest value at 120 min. The photocatalyst cleavage of the aromatic ring of the dye molecules is thought to cause a decrease in absorption peaks, which leads to the decomposition of the RhB dye [31].

The pH of the solution had a significant impact on the efficiency of the photocatalytic reactions (Fig. 5(a)). The free radicals attacked the dye molecules and caused them to degrade over time. Because of the electrostatic interaction between the negatively charged material surface (from the proton separation process) and the predominant positively charged dye cation at pH 2, the

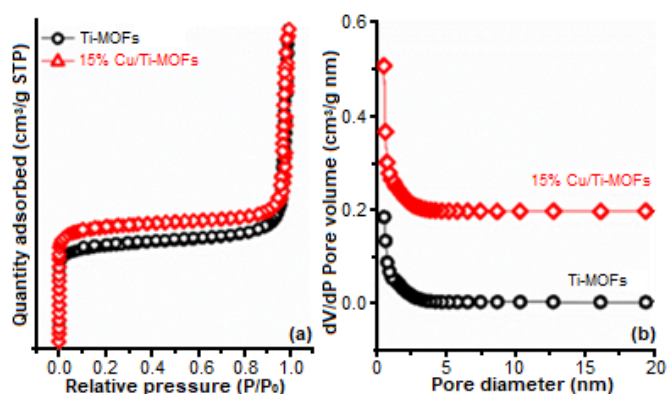


Fig 2. Adsorption-desorption isotherms of NH_2 -Ti-MOFs and 15% Cu/Ti-MOFs

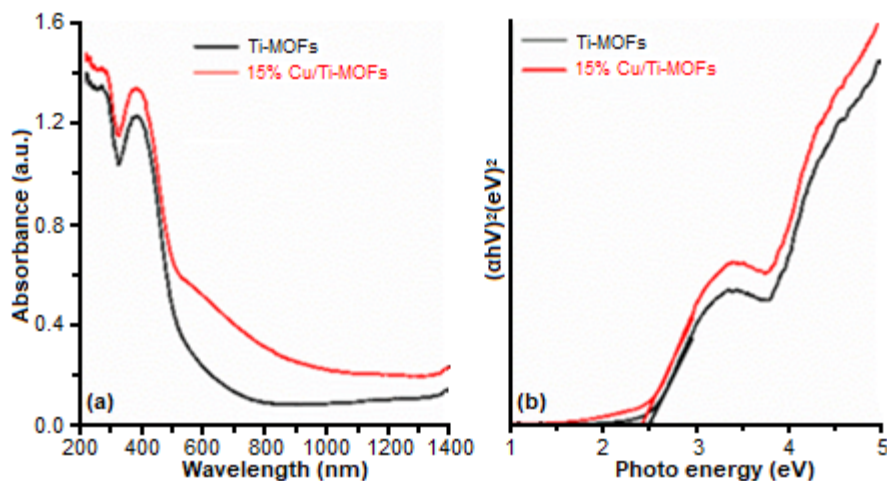


Fig 3. UV-Vis DRS (A) and Tauc plot (B) of NH_2 -Ti-MOFs and 15% Cu/Ti-MOFs

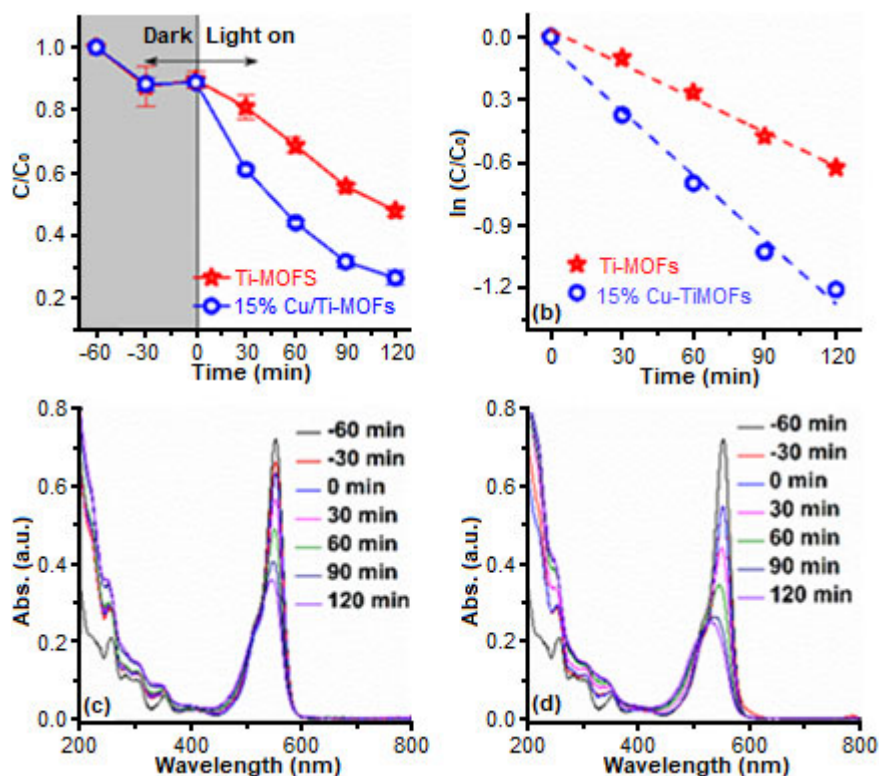


Fig 4. The removal efficiency of Rhodamine B (a) using different catalysts under visible light irradiation in the presence of H_2O_2 and (b) Pseudo first-order kinetic of the degradation process, (c, d) UV-Vis absorption spectra of RhB with respect to irradiation time over NH_2 -Ti-MOFs and 15% Cu/Ti-MOFs, respectively

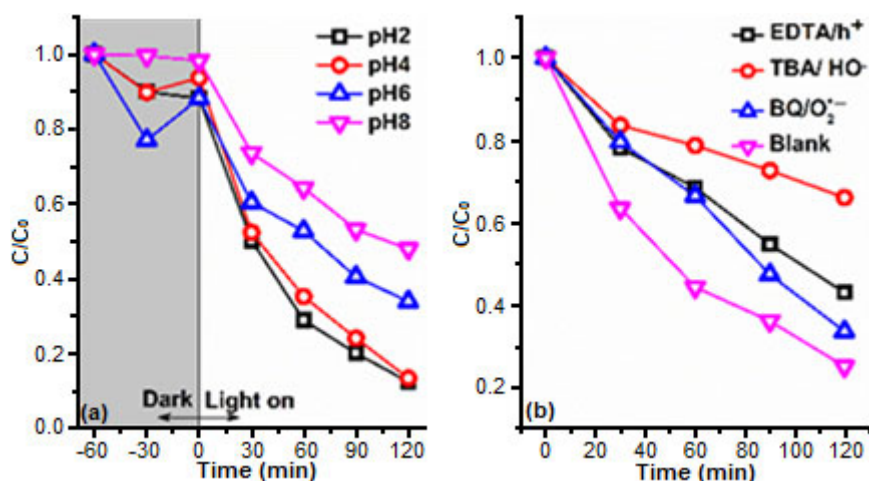


Fig 5. The effect of pH solution (a) and photocatalyst mechanism of 15% Cu/Ti-MOFs (b)

the photochemical degradation efficiency increased sharply, resulting in a sharp increase in absorbance as well as causing the photochemical reaction. When the pH rises above 8, RhB is deprotonated, and its zwitterion is formed. Furthermore, photochemical degradation was inhibited

because the hydroxyl ions competed with the RhB molecules for adsorption on the catalyst surface. This finding is consistent with the findings of Zhao et al. [32].

Reactive radicals ($\cdot OH$, $O_2^{\cdot -}$, h^+) are produced during the irradiation process and are responsible for

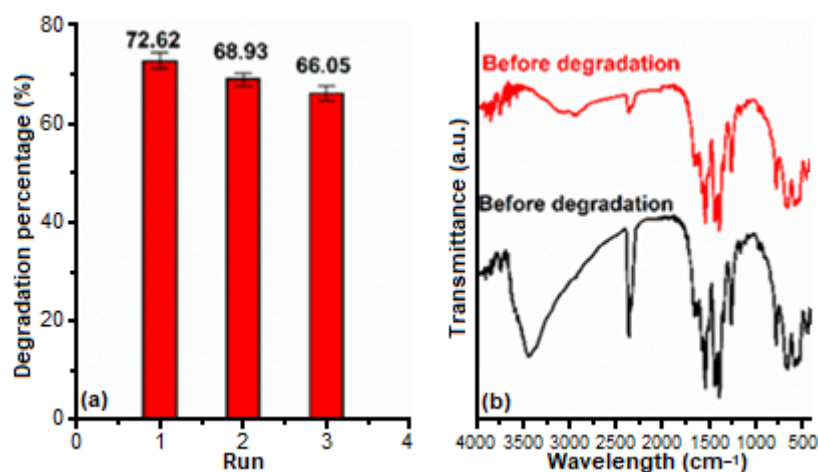


Fig 6. The reliability test of the degradation of RhB over 15% Cu/Ti-MOFs (a), FTIR spectra of 15% Cu/Ti-MOFs before and after degradation performance (b)

dye degradation. Trapping experiments were used to determine which radical was dominant. According to Fig. 5(b), the final degradation efficiency changed almost noticeably after 2 h of visible light irradiation when added with 1 mM TBA and 1 mM EDTA-2Na. Hence, $\cdot\text{OH}$ and h^+ were predominantly responsible for RhB degradation.

To investigate the stability of the photocatalyst, recycling experiments of 15% Cu/Ti-MOFs were performed under the same conditions. Fig. 6(a) depicts the photodegradation of RhB after three runs. The removal of RhB decreased from 72.62% to 66.05%, indicating that the catalyst can be used repeatedly with no discernible variation in photocatalytic performance. The FTIR spectra (Fig. 6(b)) of fresh and used catalyst (used three-times) proved the stability of 15% Cu/Ti-MOFs after the 3rd -run. The organic linkers C-C and N-H bonds bending vibrations were visible in the FTIR spectra of 15% Cu/Ti-MOFs, with peaks at 1500 and 1620 cm^{-1} , respectively [33-34]. Furthermore, the peaks at 1245 and 1414 cm^{-1} are associated with a Ti-O framework's bending and symmetric stretching [35]. According to this study, the organic linker's -COOH group was directly attached to the Ti-oxo cluster.

■ CONCLUSION

NH_2 -Ti-MOFs and 15% Cu/Ti-MOFs were successfully prepared via the solvothermal method and were used to degrade RhB dye efficiently. Compared to the individual Ti-MOFs, 15% Cu/Ti-MOFs exhibited

enhanced photocatalytic activity for RhB degradation. The promoted electron transfer by the $\text{Cu}^{2+}/\text{Cu}^+$ and $\text{Ti}^{4+}/\text{Ti}^{3+}$ redox cycles and the efficient separation of photo-excited electron-hole pairs by introducing H_2O_2 can be attributed to the accelerated photocatalytic degradation of RhB. The prepared 15% Cu/Ti-MOFs also demonstrated good reusability and stability. Further investigation revealed that the principal active species in the degradation process were hydroxyl radicals and holes. The 15% as-synthesized Cu/Ti-MOFs showed promise in the removal of organic contaminants from wastewater.

■ ACKNOWLEDGMENTS

This research was funded by the Center of Science and Technology Development for Youth, Ho Chi Minh City Communist Youth Union, Vietnam (No. 33/2020/HĐ-KHCN-VU).

■ REFERENCES

- [1] Wang, M., Yang, L., Guo, C., Liu, X., He, L., Song, Y., Zhang, Q., Qu, X., Zhang, H., Zhang, Z., and Fang, S., 2018, Bimetallic Fe/Ti-based metal-organic framework for persulfate-assisted visible light photocatalytic degradation of Orange II, *ChemistrySelect*, 3 (13), 3664-3674.
- [2] Vieira, Y., Leichtweis, J., Foletto, E.L., and Silvestri, S., 2020, Reactive oxygen species-induced heterogeneous photocatalytic degradation of

- organic pollutant rhodamine B by copper and zinc aluminate spinels, *J. Chem. Technol. Biotechnol.*, 95 (3), 791–797.
- [3] Tang, S.K., Teng, T.T., Alkarkhi, A.F.M., and Li, Z., 2012, Sonocatalytic degradation of rhodamine B in aqueous solution in the presence of TiO₂ coated activated carbon, *APCBEE Procedia*, 1, 110–115.
- [4] Shi, L., Wang, T., Zhang, H., Chang, K., Meng, X., Liu, H., and Ye, J., 2015, An amine-functionalized iron(III) metal-organic framework as efficient visible-light photocatalyst for Cr(VI) reduction, *J. Ye, Adv. Sci.*, 2 (3), 1500006.
- [5] Wu, Y.Y., Yang, C.X., and Yan, X.P., 2014, Fabrication of metal-organic framework MIL-88B films on stainless steel fibers for solid-phase microextraction of polychlorinated biphenyls, *J. Chromatogr. A*, 1334, 1–8.
- [6] Lin, K.Y.A., Chang, H.A., and Hsu, C.J., 2015, Iron-based metal-organic framework, MIL-88A, as a heterogeneous persulfate catalyst for decolorization of Rhodamine B in water, *RSC Adv.*, 5 (41), 32520–32530.
- [7] Li, H., Wang, K., Sun, Y., Lollar, C.T., Li, J., and Zhou, H.C., 2018, Recent advances in gas storage and separation using metal-organic frameworks, *Mater. Today*, 21 (2), 108–121.
- [8] Solanki, V.A., and Borah, B., 2019, Ranking of metal-organic frameworks (MOFs) for separation of hexane isomers by selective adsorption, *Ind. Eng. Chem. Res.*, 58 (43), 20047–20065.
- [9] Wang, L., Zheng, M., and Xie, Z., 2018, Nanoscale metal-organic frameworks for drug delivery: A conventional platform with new promise, *J. Mater. Chem. B*, 6 (5), 707–717.
- [10] Nguyen, H.T.T., Dinh, V.P., Phan, Q.A.N., Tran, V.A., Doan, V.D., Lee, T., and Nguyen, T.D., 2020, Bimetallic Al/Fe metal-organic framework for highly efficient photo-Fenton degradation of rhodamine B under visible light irradiation, *Mater. Lett.*, 279, 128482.
- [11] Kim, S.N., Kim, J., Kim, H.Y., Cho, H.Y., and Ahn, W.S., 2013, Adsorption/catalytic properties of MIL-125 and NH₂-MIL-125, *Catal. Today*, 204, 85–93.
- [12] Gómez-Avilés, A., Muelas-Ramos, V., Bedia, J., Rodríguez, J.J., and Belver, C., 2020, Thermal post-treatments to enhance the water stability of NH₂-MIL-125(Ti), *Catalysts*, 10 (6), 603.
- [13] Remiro-Buenamañana, S., Cabrero-Antonino, M., Martínez-Guanter, M., Álvaro, M., Navalón, S., and García, H., 2019, Influence of co-catalysts on the photocatalytic activity of MIL-125(Ti)-NH₂ in the overall water splitting, *Appl. Catal., B*, 254, 677–684.
- [14] Zhao, Y., Cai, W., Chen, J., Miao, Y., and Bu, Y., 2019, A highly efficient composite catalyst constructed from NH₂-MIL-125(Ti) and reduced graphene oxide for CO₂ photoreduction, *Front. Chem.*, 7, 789.
- [15] Hlophe, P.V., Mahlalela, L.C., and Dlamini, L.N., 2019, A composite of platelet-like orientated BiVO₄ fused with MIL-125(Ti): Synthesis and characterization, *Sci. Rep.*, 9 (1), 10044.
- [16] Rani, S., Aggarwal, M., Kumar, M., Sharma, S., and Kumar, D., 2016, Removal of methylene blue and rhodamine B from water by zirconium oxide/graphene, *Water Sci.*, 30 (1), 51–60.
- [17] Sun, D., Liu, W., Fu, Y., Fang, Z., Sun, F., Fu, X., Zhang, Y., and Li, Z., 2014, Noble metals can have different effects on photocatalysis over metal-organic frameworks (MOFs): A case study on M/NH₂-MIL-125(Ti) (M=Pt and Au), *Chem. Eur. J.*, 20 (16), 4780–4788.
- [18] Wang, D., and Li, Z., 2016, Coupling MOF-based photocatalysis with Pd catalysis over Pd@MIL-100(Fe) for efficient N-alkylation of amines with alcohols under visible light, *J. Catal.*, 342, 151–157.
- [19] Su, Y., Zhang, Z., Liu, H., and Wang, Y., 2017, Cd_{0.2}Zn_{0.8}S@UiO-66-NH₂ nanocomposites as efficient and stable visible-light-driven photocatalyst for H₂ evolution and CO₂ reduction, *Appl. Catal., B*, 200, 448–457.
- [20] Liang, R., Shen, L., Jing, F., Qin, N., and Wu, L., 2015, Preparation of MIL-53(Fe)-reduced graphene oxide nanocomposites by a simple self-assembly strategy for increasing interfacial contact: Efficient visible-light photocatalysts, *ACS Appl. Mater. Interfaces*, 7 (18), 9507–9515.

- [21] Ao, D., Zhang, J., and Liu, H., 2018, Visible-light-driven photocatalytic degradation of pollutants over Cu-doped NH₂-MIL-125(Ti), *J. Photochem. Photobiol., A*, 364, 524–533.
- [22] Gómez-Avilés, A., Peñas-Garzón, M., Bedia, J., Dionysiou, D.D., Rodríguez, J.J., and Belver, C., 2019, Mixed Ti-Zr metal-organic-frameworks for the photodegradation of acetaminophen under solar irradiation, *Appl. Catal., B*, 253, 253–262.
- [23] Hanna, L., Long, C.L., Zhang, X., and Lockard, J.V., 2020, Heterometal incorporation in NH₂-MIL-125(Ti) and its participation in the photoinduced charge-separated excited state, *Chem. Commun.*, 56 (78), 11597–11600.
- [24] Sun, D., Liu, W., Qiu, M., Zhang, Y., and Li, Z., 2015, Introduction of a mediator for enhancing photocatalytic performance via post-synthetic metal exchange in metal-organic frameworks (MOFs), *Chem. Commun.*, 51 (11), 2056–2059.
- [25] Zhu, S.R., Liu, P.F., Wu, M.K., Zhao, W.N., Li, G.C., Tao, K., Yi, F.Y., and Han, L., 2016, Enhanced photocatalytic performance of BiOBr/NH₂-MIL-125(Ti) composite for dye degradation under visible light, *Dalton Trans.*, 45 (43), 17521–17529.
- [26] Muelas Ramos, V., Belver, C., Rodríguez, J.J., and Bedia, J., 2021, Synthesis of noble metal-decorated NH₂-MIL-125 titanium MOF for the photocatalytic degradation of acetaminophen under solar irradiation, *Sep. Purif. Technol.*, 272, 118896.
- [27] Yuan, X., Wang, H., Wu, Y., Zeng, G., Chen, X., Leng, L., Wu, Z., and Li, H., 2016, One-pot self-assembly and photoreduction synthesis of silver nanoparticle-decorated reduced graphene oxide/MIL-125(Ti) photocatalyst with improved visible-light photocatalytic activity, *Appl. Organomet. Chem.*, 30 (5), 289–296.
- [28] Karthik, P., Vinoth, R., Zhang, P., Choi, W., Balaraman, E., and Neppolian, B., 2018, π - π Interaction between metal-organic framework and reduced graphene oxide for visible-light photocatalytic H₂ production, *ACS Appl. Energy Mater.*, 1 (5), 1913–1923.
- [29] Hu, S., Liu, M., Li, K., Zuo, Y., Zhang, A., Song, C., Zhang, G., and Guo, X., 2014, Solvothermal synthesis of NH₂-MIL-125(Ti) from circular plate to octahedron, *CrystEngComm*, 16 (41), 9645–9650.
- [30] Fiaz, M., Kashif, M., Majeed, S., Ashiq, M.N., Farid, M.A., and Athar, M., 2019, Facile fabrication of highly efficient photoelectrocatalysts M_xO_y@NH₂-MIL-125(Ti) for enhanced hydrogen evolution reaction, *ChemistrySelect*, 4 (23), 6996–7002.
- [31] Jia, K., Wang, Y., Pan, Q., Zhong, B., Luo, Y., Cui, G., Guo, X., and Sun, X., 2019, Enabling the electrocatalytic fixation of N₂ to NH₃ by C-doped TiO₂ nanoparticles under ambient conditions, *Nanoscale Adv.*, 1 (3), 961–964.
- [32] Zhao, H., Zhang, Y., Li, G., Tian, F., Tang, H., and Chen, R., 2016, Rhodamine B-sensitized BiOCl hierarchical nanostructure for methyl orange photodegradation, *RSC Adv.*, 6 (10), 7772–7779.
- [33] Shen, L., Liang, S., Wu, W., Liang, R., and Wu, L., 2013, Multifunctional NH₂-mediated zirconium metal-organic framework as an efficient visible-light-driven photocatalyst for selective oxidation of alcohols and reduction of aqueous Cr(VI), *Dalton Trans.*, 42 (37), 13649–13657.
- [34] Liang, R., Shen, L., Jing, F., Wu, W., Qin, N., Lin, R., and Wu, L., 2015, NH₂-mediated indium metal-organic framework as a novel visible-light-driven photocatalyst for reduction of the aqueous Cr(VI), *Appl. Catal., B*, 162, 245–251.
- [35] Yin, S., Chen, Y., Hu, Q., Li, M., Ding, Y., Di, J., Xia, J., and Li, H., 2020, Construction of NH₂-MIL-125(Ti) nanoplates modified Bi₂WO₆ microspheres with boosted visible-light photocatalytic activity, *Res. Chem. Intermed.*, 46 (7), 3311–3326.